PAPER

Probing the shear modulus of two-dimensional multiplanar nanostructures and heterostructures

T. Mukhopadhyay, [iD] *[a] A. Mahata,[b] S. Adhikari[c] and M. Asle Zaeem [iD] [b]

Generalized high-fidelity closed-form formulae have been developed to predict the shear modulus of hexagonal graphene-like monolayer nanostructures and nano-heterostructures based on a physically insightful analytical approach. Hexagonal nano-structural forms (top view) are common for nanomaterials with monoplanar (such as graphene and hBN) and multiplanar (such as stanene and MoS_2) configurations. However, a single-layer nanomaterial may not possess a particular property adequately, or multiple desired properties simultaneously. Recently, a new trend has emerged to develop nano-heterostructures by assembling multiple monolayers of different nanostructures to achieve various tunable desired properties simultaneously. Shear modulus assumes an important role in characterizing the applicability of different two-dimensional nanomaterials and heterostructures in various nanoelectromechanical systems such as determining the resonance frequency of vibration modes involving torsion, wrinkling and rippling behavior of two-dimensional materials. We have developed mechanics-based closed-form formulae for the shear modulus of monolayer nanostructures and multi-layer nano-heterostructures. New results of shear modulus are presented for different classes of nanostructures (graphene, hBN, stanene and MoS_2) and nano-heterostructures (graphene–hBN, graphene–MoS_2, graphene–stanene and stanene–MoS_2), which are categorized on the basis of fundamental structural configurations. The numerical values of shear modulus are compared with the results from the scientific literature (as available) and separate molecular dynamics simulations, wherein a good agreement is noticed. The proposed analytical expressions will enable the scientific community to efficiently evaluate shear modulus of a wide range of nanostructures and nanoheterostructures.

1. Introduction

A mechanics-based analytical approach is presented to derive generalized closed-form formulae for the effective shear modulus of hexagonal multiplanar nano-structures and nano-heterostructures. With the feasible isolation of single layer carbon atoms, known as graphene,[1,2] the fascinating and unprecedented properties of this monolayer nanostructure had initiated intense research in the exploration of prospective alternative two-dimensional and quasi-two-dimensional materials that could possess exciting electronic, optical, thermal, chemical and mechanical characteristics.[3–9] It is important to investigate these materials at the nano-scale as most of the interesting characteristics are in the atomic scale and monolayer forms.[10] Over the span of the last decade the interest in such two-dimensional nanomaterials has expanded

from hBN, BCN, graphene oxides to chalcogenides (MoS_2 and $MoSe_2$) and other quasi-two-dimensional materials like stanene, phosphorene, silicene, germanene, borophene *etc.*[11–15] Among different such materials, as discussed above, the hexagonal nanostructural form is a prominent structural configuration.[4,16] From a structural view-point, monolayer nanostructures can be of either monoplanar (where all the atoms are in a single plane such as graphene and hBN) or multiplanar (where the constituent atoms lie in multiple planes such as stanene and MoS_2) configurations (refer to sub-section 2.1 for a detailed description of monoplanar and multiplanar nanostructures).

Despite considerable advancement in two-dimensional materials research, it has been realized that a single-layer nanomaterial may not possess a particular property adequately, or multiple desired properties simultaneously. Recently a new trend has emerged to develop nano-heterostructures by assembling multiple monolayers of different nanostructures to achieve various tunable desired properties simultaneously.[17–20] Although the monolayers of quasi-two-dimensional materials have a hexagonal lattice nano-structure (top-view) in common, their out-of-plane lattice characteristics

[a]*Department of Engineering Science, University of Oxford, Oxford, UK.*
E-mail: tanmoy.mukhopadhyay@eng.ox.ac.uk
[b]*Department of Materials Science and Engineering, Missouri University of Science and Technology, Rolla, USA*
[c]*College of Engineering, Swansea University, Swansea, UK*

are quite different. Subsequently, these materials exhibit significantly different mechanical and electronic properties. For example, transition metal dichalcogenides such as MoS_2 show exciting electronic and piezoelectric properties, but their low in-plane mechanical strength is a constraint for any practical application. In contrast, graphene possesses strong in-plane mechanical properties. Moreover, graphene is extremely weak in the out-of-plane direction with a very low bending modulus, whereas the bending modulus of MoS_2 is comparatively much higher, depending on its respective single-layer thickness.[21] Having noted that graphene and MoS_2 possess such complementary physical properties, it is a quite rational attempt to combine these two materials in the form of a graphene–MoS_2 heterostructure, which could exhibit the desired level of electronic properties and in-plane as well as out-of-plane strengths. Besides intense research on different two-dimensional hexagonal nano-structural forms, recently the development of novel application-specific heterostructures has started receiving considerable attention from the scientific community due to the considerable prospect of combining different single layer materials by intelligent and intuitive ways to achieve several such desired physical and chemical properties.[22–30]

For understanding the structural performance of nanostructures and nano-heterostructures (intended to be utilized as nanoelectromechanical systems such as resonators or nanosensors) from a mechanical strength view-point, it is of utmost importance to evaluate their Young's moduli, Poisson's ratios and shear moduli. While closed-form analytical expressions have been reported in the literature for Young's moduli and Poisson's ratios of multiplanar structural forms and nano-heterostructures,[31,32] there are no such efficient formulae available yet for the shear modulus of nanostructure and nano-heterostructures. Shear modulus assumes a vital role in evaluating the resonance frequency of vibration modes involving torsion. Such torsional modes have been reported to have advantages over flexural modes due to the absence of thermoelastic loss leading to an improvement in mechanical quality factors and device sensitivity. Shear deformation is also important in characterizing the wrinkling and rippling behaviour of two-dimensional materials that controls the charge carrier scattering properties and electron mobility.[33]

The common computational approaches to investigate two-dimensional nanomaterials are first principles studies/ *ab initio*,[34–39] molecular dynamics[40] and molecular mechanics,[41] which are capable of reproducing the results of experimental analysis. First principles studies/*ab initio* and molecular dynamics based material characterization approaches are normally expensive and time consuming. Moreover, the availability of interatomic potentials can be a practical barrier for carrying out molecular dynamics simulation for nano-heterostructures, which consist of multiple materials. A mechanics-based analytical approach for evaluating elastic moduli is computationally very efficient, yet produces accurate results. Analytical models leading to efficient closed-form formulae have been presented by many researchers for materials with

monoplanar hexagonal nano-structures,[42–45] while the shear modulus of multiplanar structures are not found to be adequately addressed. Research in the field of nano-heterostructures is still in a very nascent stage and investigations on the elastic properties of such built-up structural forms are very scarce in the literature,[22,23,46] wherein a predominant approach for evaluating elastic moduli is expensive molecular dynamics simulation. To achieve the full potential of such nano-scale built-up structural forms, it is essential to develop computationally efficient closed-form formulae for the effective elastic properties of nano-heterostructures that can serve as a ready reference for researchers without the need for conducting expensive and time consuming molecular dynamics simulation or laboratory experiments. Since the shear modulus of different two-dimensional nanomaterials and heterostructures is very scarce in the literature, there exists a strong rationale to develop a generalized analytical model leading to efficient and closed-form, yet high fidelity expressions for obtaining the shear modulus of such natural and artificial nanomaterials.

The aim of the present paper is to cater to the need for developing an efficient physics-based framework that can obtain the shear modulus of a wide range of monolayer nano-structures (monoplanar and multiplanar) and nano-heterostructures (with any stacking configuration). This article hereafter is organized as follows: analytical formulae for the shear modulus of nano-scale materials with multiplanar hexagonal nano-structures and nano-heterostructures are derived in section 2; results and relevant discussions on the developed analytical approach is provided in section 3 along with validation of the developed formulae for four different single-layer materials belonging to four different classes (graphene, hBN, stanene and MoS_2) and four different heterostructures belonging to three categories (graphene–hBN, stanene–MoS_2, graphene–stanene and graphene–MoS_2); a summary of the important observations made from the results and perspective of this work in the context of contemporary research is provided in section 4 and finally conclusion and scope of future research based on this work are presented in section 5.

2. Shear modulus of hexagonal nanostructures and heterostructures

Generalized closed-form mechanics-based formulae for the shear modulus of hexagonal nanostructures (applicable to both monoplanar and multiplanar structural forms) and nano-heterostructures (applicable to any number of layers and stacking sequence) are developed in this section. After a concise discussion of the structural classification of nanomaterials, the equivalent elastic properties of atomic bonds are described; thereby the closed-form expressions of shear modulus are derived. The approach for obtaining the equivalent elastic properties of atomic bonds is well-established in the scientific literature.[32,41,43,47,48] Therefore, the main contribution of

this work lies in the development of the analytical formulae for the shear modulus of monoplanar and multiplanar hexagonal nanostructures and nano-heterostructures. In this context, it can be noted that the mechanics of the honeycomb-like structural form is investigated extensively at the micro- and macro-scale based on the principles of structural mechanics.[49–55]

2.1. Classification of hexagonal nanomaterials based on structural configuration

On the basis of structural configuration, monolayer two-dimensional materials can be classified into four different classes as shown in Fig. 1(e–h).[32] For example, graphene[42] con-

sists of a single type of atom (carbon) to form a hexagonal honeycomb-like lattice structure in one single plane, while there is a different class of materials that possess a hexagonal monoplanar nanostructure with different constituent atoms such as hBN,[44] BCN[56] etc. Unlike these monoplanar hexagonal nanostructures, there are plenty of other materials having the constituent atoms placed in multiple planes to form a hexagonal top view. Such multiplanar hexagonal nanostructures may consist of either a single type of atom (such as stanene,[57] silicene,[58] germanene,[58] phosphorene,[59] borophene[60] etc.), or different atoms (such as MoS_2,[61–63] WS_2,[64] $MoSe_2$,[65] WSe_2,[64] $MoTe_2$[66] etc.). However, from a view-point of mechanics, two separate categories are required to recognise: monoplanar structures (where all the constituent atoms are in a single
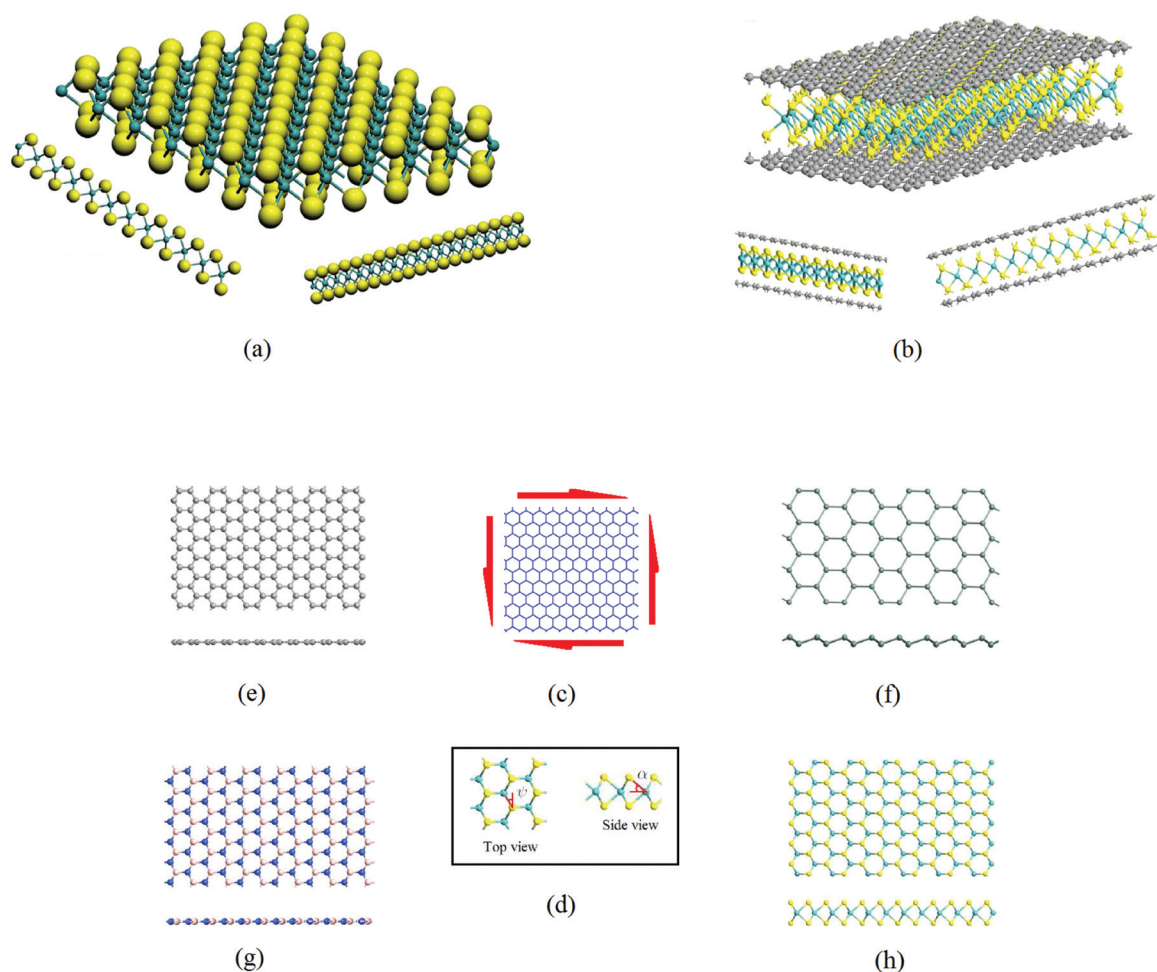

Fig. 1 (a) Three dimensional view of multiplanar hexagonal nano-structures along with side views from two mutually perpendicular directions. (b) Three dimensional view of nano-heterostructure structures (having three layers consisting of a multiplanar layer sandwiched between two monoplanar layers at the top and bottom) along with side views from two mutually perpendicular directions. (c) A typical representation of hexagonal two-dimensional nanostructures subjected to in-plane shear stress. (d) Top and side views of a generalized hexagonal nanostructural form. (e) Top and side views of single-layer hexagonal nanostructures where all the constituent atoms are the same and they are in a single plane (class I: *e.g.* graphene). (f) Top and side views of single-layer hexagonal nanostructures where the constituent atoms are the same but they are in two different planes (class II: *e.g.* silicene, germanene, phosphorene, stanene, and borophene). (g) Top and side views of single-layer hexagonal nanostructures where the constituent atoms are not the same but they are in a single plane (class III: *e.g.* hBN and BCN). (h) Top and side views of single-layer hexagonal nanostructures where the constituent atoms are not the same and they are in two different planes (class IV: *e.g.* MoS_2, WS_2, $MoSe_2$, WSe_2, and $MoTe_2$).

plane, such as graphene and hBN) and multiplanar structures (where all the constituent atoms are in different planes, such as stanene and MoS_2). This is because of the fact that the equivalent properties of the bonds are important in evaluating the elastic properties of materials, rather than the similarity or dissimilarity of two adjacent atoms. It can be noted in this context that the monoplanar structural form can be treated as a special case of multiplanar structures. The top view and side view of a general multiplanar hexagonal nanostructure are shown in Fig. 1(d). From the figure, it is evident that a multiplanar structure reduces to a monoplanar form when the out-of-plane angle becomes zero (*i.e.* $\alpha = 0$).

From a structural perspective, the hexagonal nano-heterostructures can be broadly classified into three categories: heterostructures containing only mono-planar nanostructures (such as graphene–hBN heterostructure[24,25,67]), heterostructures containing both mono-planar and multi-planar nanostructures (such as graphene–MoS_2 heterostructure,[21,23] graphene–stanene heterostructure,[26] phosphorene–graphene heterostructure,[68] phosphorene–hBN heterostructure,[68] and multi-layer graphene–hBN–TMDC heterostructure[28]) and heterostructures containing only multi-planar nanostructures (such as stanene–MoS_2 heterostructure[27] and MoS_2–WS_2 heterostructure[22]).

2.2. Mechanical equivalence of atomic bonds

For the atomic level behaviour of nano-scale materials, the effective interatomic potential energy can be evaluated as a sum of various individual energy components related to

bonding and non-bonding interactions.[41] Total strain energy (E) consists of contributions from bending of bonds (E_b), bond stretching (E_s), torsion of bonds (E_t) and energies associated with non-bonded terms (E_{nb}) such as van der Waals attraction, core repulsions and coulombic energy:

$$E = E_s + E_b + E_t + E_{nb} \tag{1}$$

However, among all the energy components, the effects of bending and stretching are predominant in the case of small deformation.[43,47] For the multiplanar hexagonal nano-structures (such as stanene and MoS_2), the strain energy pertaining to bending consists of two components: in-plane component (E_{bI}) and out-of-plane component (E_{bO}). The predominant deformation mechanisms for a multiplanar nanostructure are depicted in Fig. 2. It can be noted that the out-of-plane component becomes zero for monoplanar nanostructures such as graphene and hBN. The total inter-atomic potential energy (E) can be expressed as

$$E = E_s + E_{bI} + E_{bO} = \frac{1}{2}k_r(\Delta l)^2 + \left(\frac{1}{2}k_\theta(\Delta \theta)^2 + \frac{1}{2}k_\theta(\Delta \alpha)^2\right) \tag{2}$$

where Δl, $\Delta \theta$ and $\Delta \alpha$ denote the change in bond length, in-plane angle and out-of-plane angle, respectively, as shown in Fig. 2. The quantities k_r and k_θ represent the force constants related to bond stretching and bending, respectively. The first term in eqn (2) corresponds to the strain energy due to stretching (E_s), while the terms within brackets represent the strain energies due to the in-plane angle (E_{bI}) and out-of-plane (E_{bO}) angle variations, respectively. The force constants of the
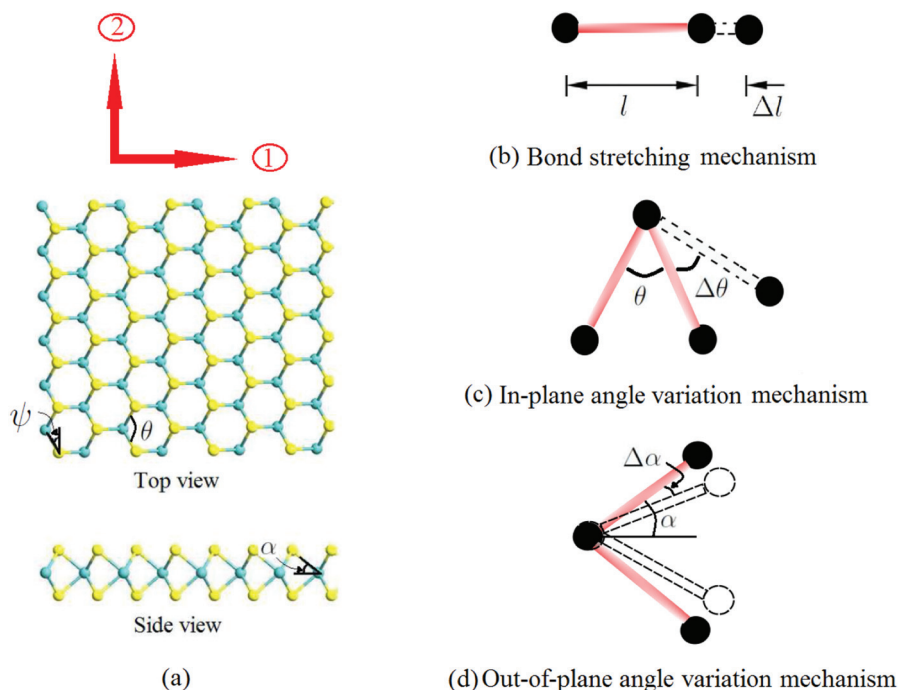

Fig. 2 (a) Top and side views of a multiplanar hexagonal nanostructure. (b) Deformation mechanism of bond stretching. (c) Deformation mechanism of in-plane (1–2 plane) angle variation. (d) Deformation mechanism of out-of-plane (normal to the 1–2 plane) angle variation.

atomic bonds (k_r and k_θ) can be expressed in the form of structural equivalence.[69] As per the standard theory of structural mechanics, the strain energy of a uniform circular beam having length l, cross-sectional area A, second moment of area I and Young's modulus E, under the application of a pure axial force N, can be expressed as

$$U_a = \frac{1}{2}\int_0^L \frac{N^2}{EA}\,dl = \frac{1}{2}\frac{N^2 l}{EA} = \frac{1}{2}\frac{EA}{l}(\Delta l)^2 \qquad (3)$$

The strain energies due to pure bending moment M causing a slope of $\Delta\phi$ at the end points of the beam[32] can be written as

$$U_b = \frac{1}{2}\int_0^L \frac{M^2}{EI}\,dl = \frac{1}{2}\frac{EI}{l}(2\Delta\phi)^2 \qquad (4)$$

Comparing eqn (3) with the expression for strain energy due to stretching (E_s) (refer to eqn (2)), it can be concluded that $k_r = \frac{EA}{l}$. For bending, it is reasonable to assume that $2\Delta\phi$ is equivalent to $\Delta\theta$ and $\Delta\alpha$ for the in-plane and out-of-plane angle variations, respectively. Thus comparing eqn (4) with the expressions for the strain energies due to in-plane (E_{bI}) and out-of-plane (E_{bO}) angle variations, the following relationship can be obtained: $k_\theta = \frac{EI}{l}$. On the basis of the established mechanical equivalence between the molecular mechanics parameters (k_r and k_θ) and structural mechanics parameters (EA and EI), the effective shear moduli of monolayer nano-structures and nano-heterostructures are obtained in the following subsections.

2.3.   Shear modulus of mono-layer quasi-two-dimensional hexagonal nanostructures

For deriving the in-plane shear modulus of multiplanar hexagonal nanostructures, the free body diagram shown in Fig. 3 is analysed. It should be noted here that the top view is shown in this figure and the individual constituent members are inclined at an angle α as described in Fig. 1(c). On analysis of the free body diagram presented in Fig. 3(b) one obtains

$$M = \frac{Fl\cos\alpha}{4} \qquad (5)$$

where $F = 2\tau l^2 \cos\psi\cos\alpha\sin\alpha$. Deflection of end A with respect to end C under the application of moment M at point A is given as

$$\delta_0 = \frac{Ml^2}{6EI} \qquad (6)$$

Thus the rotation of joint A can be expressed as

$$\phi = \frac{\delta_0}{l} = \frac{Fl^2\cos\alpha}{24EI} \qquad (7)$$

Deformation of point D′ in the direction of F due to the rotation of joint A is given by

$$\delta_r = \frac{1}{2}\phi l = \frac{Fl^3\cos\alpha}{48EI} \qquad (8)$$

The bending deformation of the member AD′ in the direction of F can be expressed as

$$\delta_b = \frac{Fl^3}{24EI} \qquad (9)$$

The total shear deformation due to the bending of the member AD′ and rotation of joint A is given by

$$u_s = \delta_b + \delta_r = \frac{Fl^3}{48EI}(\cos\alpha + 2) \qquad (10)$$

The axial deformation of members AB and AC caused by the force S will also contribute to the total shear deformation, where $S = \tau l^2 \sin\alpha\cos\alpha(1 + \sin\psi)$. Comparing the expression of τ, obtained from the expressions of F and S

$$S = \frac{F(1 + \sin\psi)}{2\cos\psi} \qquad (11)$$

The axial deformation of the member AB can be expressed as (refer to Fig. 2(a) for the in-plane and out-of-plane angles ψ and α, respectively. Fig. 3(b) shows the application of two forces S and $\frac{F}{2}$ on the member AB)

$$\delta_a = \frac{\left(S\sin\psi + \frac{F}{2}\cos\psi\right)\cos\,\alpha l\cos\alpha\sin\psi}{AE}$$
$$= \frac{Fl\sin\psi(1 + \sin\,\psi)\cos^2\alpha}{2AE\cos\psi} \qquad (12)$$

Based on the force components shown in the free body diagrams of Fig. 3(b), the axial deformation of the members AB
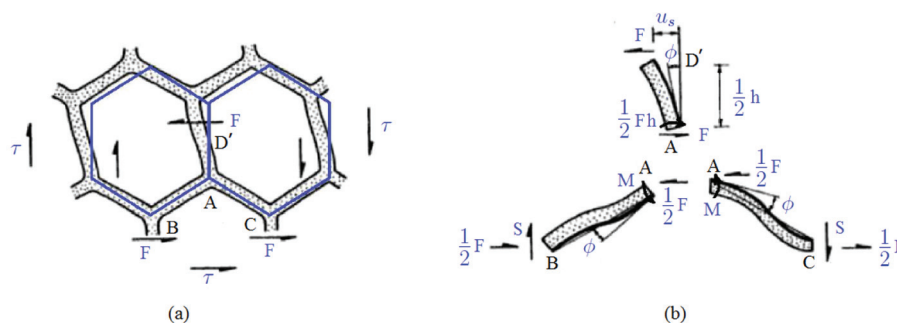

Fig. 3   Top view of a multi-planar hexagonal lattice for deriving the in-plane shear modulus.

and AC would have the same numerical value, but of opposite nature. Thus the total shear strain component caused by the axial deformation of the members AB and AC can be expressed as

$$\gamma_a = \frac{2\delta_a}{2l \cos \psi \cos \alpha} \tag{13}$$

The shear strain component caused by the bending deformation of the member AD′ and rotation of joint A is given by

$$\gamma_b = \frac{u_s}{l(1 + \sin \psi)\cos \alpha} \tag{14}$$

Substituting the expressions of δ_a and u_s from eqn (12) and (10), respectively, the total shear strain caused by bending and axial deformations for an entire hexagonal unit (as shown in Fig. 3(a)) can be obtained as[49]

$$\gamma = 2(\gamma_a + \gamma_b)$$
$$= \tau l^2 \cos \psi \cos \alpha \sin \alpha \left(\frac{\sin \psi (1 + \sin \psi)}{AE \cos^2 \psi} + \frac{l^2 (\cos \alpha + 2)}{6EI(1 + \sin \psi)\cos \alpha} \right) \tag{15}$$

Replacing the structural mechanics parameters EI and AE by the molecular mechanics parameters k_θ and k_r, respectively $(k_r = \frac{EA}{l}$ and $k_\theta = \frac{EI}{l})$ in the above equation, the expression for in-plane shear modulus can be expressed as

$$G_{12} = \frac{\tau}{\gamma}$$
$$= \frac{k_r k_\theta \cos \psi (1 + \sin \psi)}{t \left(k_\theta \sin \psi (1 + \sin \psi)^2 \cos \alpha + \frac{k_r l^2}{6} \cos^2 \psi (\cos \alpha + 2) \right)} \tag{16}$$

In the above expression $\psi = 90° - \frac{\theta}{2}$, where θ is the bond angle as shown in Fig. 2(a).

2.4. Effective shear modulus of multi-layer hexagonal nano-heterostructures

The equivalent shear modulus of the nano-heterostructures is derived based on a multi-stage bottom-up idealization scheme as depicted in Fig. 4. In the first stage, the effective shear modulus of each individual layer is determined based on a mechanics-based approach using the mechanical equivalence of bond properties as described in the preceding subsection. Thus the multi-layer heterostructure can be idealized as a

layered plate-like structural element with respective effective shear modulus and geometric dimensions (such as thickness) of each layer. Each of the layers is considered to be bonded perfectly with the adjacent layers. The equivalent shear modulus of the whole nano-heterostructure is determined based on force equilibrium and deformation compatibility based conditions in the final stage.

Fig. 5 shows the typical representation of an idealized three-layer heterostructure with the in-plane shear stress applied in the 1–2 plane. From the condition of force equilibrium, the total shear force should be equal to the summation of the shear force component shared by each of the constituting layers. Thus considering a heterostructure with n number of layers

$$\tau t L = \sum_{i=1}^{n} \tau_i t_i L \tag{17}$$

From the definition of the shear modulus, the above expression can be written as

$$G_{12}\gamma t = \sum_{i=1}^{n} G_{12i}\gamma_i t_i \tag{18}$$

where G_{12} and γ are the effective shear modulus and the shear strain, respectively, for the entire heterostructure. G_{12i} and γ_i represent the effective shear modulus and the shear strain of the ith layer, respectively. As each of the layers is considered to be perfectly bonded with the adjacent layers, the deformation compatibility condition yields: $\gamma = \gamma_i$, $\in[1, n]$. Thus eqn (18) and (16) give the expression of the in-plane shear modulus for the entire heterostructure as

$$G_{12} = \frac{1}{t}\sum_{i=1}^{n} G_{12i}t_i$$
$$= \frac{1}{t}\sum_{i=1}^{n} \frac{k_{ri}k_{\theta i} \cos \psi_i (1 + \sin \psi_i)}{\left(k_{\theta i} \sin \psi_i (1 + \sin \psi_i)^2 \cos \alpha_i + \frac{k_{ri} l_i^2}{6} \cos^2 \psi_i (\cos \alpha_i + 2) \right)} \tag{19}$$

The subscript i in the above expression of G_{12} indicates the molecular mechanics and structural (/geometrical) properties corresponding to the ith layer. Here t denotes the total thickness of the heterostructure.
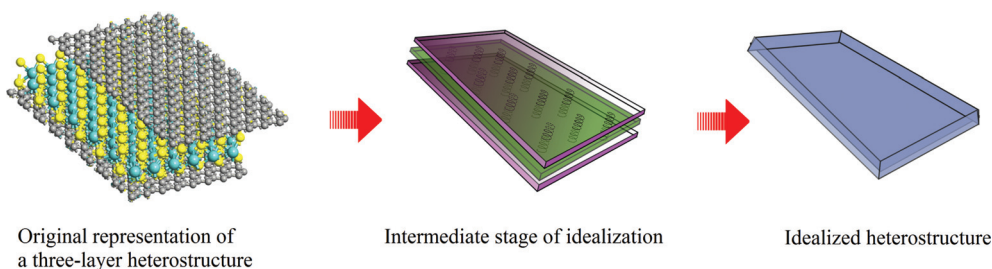

Fig. 4 Idealization scheme for the analysis of a typical three-layer nano-heterostructure.

Original representation of a three-layer heterostructure

Intermediate stage of idealization
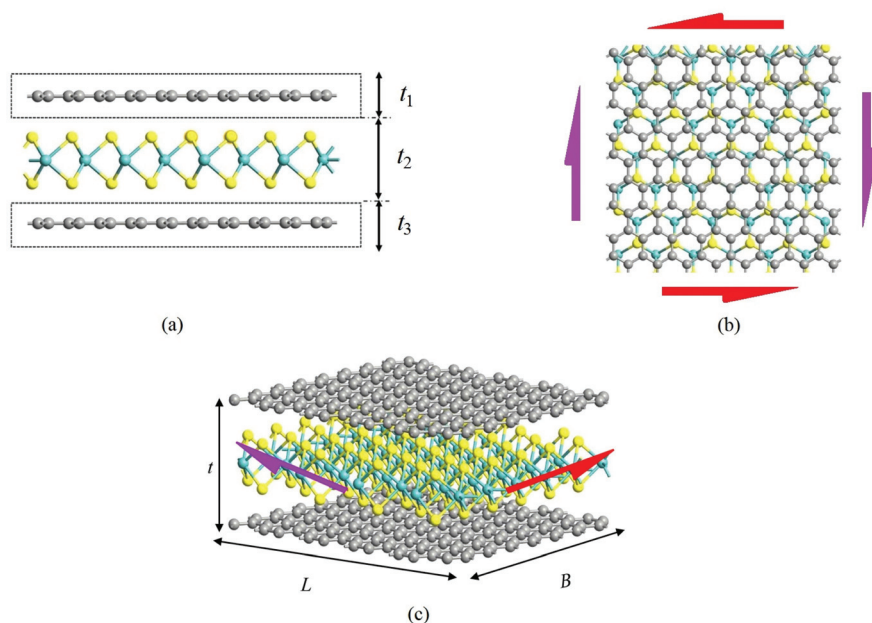
Idealized heterostructure

Fig. 5 (a) Side view of a typical three-layer heterostructure. (b) Application of shear stress in nano-heterostructures (top view). (c) Application of shear stress in nano-heterostructures (three-dimensional view).

2.5. Remark 1: non-dimensionalization of shear modulus for monolayer nanostructures

The physics based analytical formulae developed in this article are capable of providing a comprehensive understanding of the behaviour of multiplanar hexagonal nano-structures. Non-dimensional quantities in physical systems can cater to an insight for a wide range of nano-scale materials. The expression for shear modulus, as presented in eqn (16), can be rewritten in terms of non-dimensional parameters as

$$\tilde{G}_{12} = \frac{\cos \psi (1 + \sin \psi)}{(\sin \psi (1 + \sin \psi)^2 \cos \alpha + 2\lambda \cos^2 \psi (\cos \alpha + 2))} \quad (20)$$

where $\lambda \left(= \frac{l^2}{12} \frac{k_r}{k_\theta}\right)$ is a non-dimensional aspect ratio measure of the bonds that is found to vary in the range of 0.4–2.8 for common materials with hexagonal nanostructures. It is interesting to note that λ reduces to $\frac{4}{3}\left(\frac{l}{d}\right)^2$ using the definitions of k_r and k_θ, where l and d are the bond length and bond diameter, respectively. Thus the parameter λ is a measure of the aspect ratio of the bonds in hexagonal nano-structures. Here $\tilde{G}_{12} = \frac{G_{12}t}{k_r}$ is the non-dimensional representation of the shear modulus. Thus the non-dimensional shear modulus depends on the aspect ratio of the bond and in-plane and out-of-plane angles. Results are presented in section 3 considering the non-dimensional quantities for in-depth mechanical characterization of hexagonal nanostructures.

2.6. Remark 2: special case for monoplanar nanostructures

For the hexagonal nanostructures with a monoplanar configuration (e.g. graphene and hBN), α becomes 0. The shear modulus for such materials can be expressed as (substituting $\alpha = 0$ in eqn (16))

$$G_{12} = \frac{k_r k_\theta \cos \psi (1 + \sin \psi)}{t\left(k_\theta \sin \psi (1 + \sin \psi)^2 + \frac{k_r l^2}{2} \cos^2 \psi\right)} \quad (21)$$

However, for regular hexagonal nano-structures (such as graphene), the bond angle (θ) is 120°. Thus replacing $\psi = 30°$, eqn (21) yields a simple expression as

$$G_{12} = \frac{2\sqrt{3} k_\theta k_r}{t(3k_\theta + k_r l^2)} \quad (22)$$

2.7. Remark 3: effective shear modulus of nano-heterostructures

The expression for the shear modulus of nano-heterostructures derived in the preceding section (eqn (19)) reduces to the expression provided for a single layer of nanostructure (eqn (16)) in the case of $n = 1$. The derived closed-form expressions for nano-heterostructures are capable of obtaining the shear modulus corresponding to any stacking sequence of the constituent layer of nano-materials, including the heterostructures consisting of multiple materials.[28] Such generalization in the derived formulae, with the advantage of being computationally efficient and easy to implement, opens up a considerable potential scope in the field of novel application-specific heterostructure development.

An advantage of the proposed bottom-up approach of considering layer-wise equivalent material properties is that it allows us to neglect the effect of lattice mismatch in evaluating the effective shear modulus for multi-layer heterostructures consisting of different materials. In the derivation of effective shear modulus of such heterostructures, the deformation compatibility conditions of the adjacent layers are satisfied. This is expected to give rise to some strain energy locally at the interfaces, which was noted in previous studies.[23] From the derived expressions it can be discerned that the numerical values of the shear modulus actually depends on the number of layers of different constituent materials rather than their stacking sequences. In the case of multi-layer nanostructures constituted of the layers of the same material (*i.e.* bulk material), it can be expected from eqn (19) that the shear modulus would reduce owing to the presence of inter-layer distances, which, in turn, increase the value of the overall thickness t.

3. Results and discussion

3.1. Equivalent bond parameters and structural configurations of nanostructures

Four different materials with hexagonal nano-structures (graphene, hBN, stanene and MoS_2) and heterostructures formed by these four materials are considered in this paper to present the results based on eqn (16) and (19). The molecular mechanics parameters and geometric properties of the bonds (k_r, k_θ, bond length in-plane and out-of-plane bond angles for different materials), which are required to obtain the shear modulus using the proposed approach, are well-documented in the scientific literature. In the case of graphene, the molecular mechanics parameters k_r and k_θ can be obtained from the literature using AMBER force field[70] as $k_r = 938$ kcal mol^{-1} nm$^{-2} = 6.52 \times 10^{-7}$ N nm^{-1} and $k_\theta = 126$ kcal mol^{-1} rad$^{-2} = 8.76 \times 10^{-10}$ N nm rad^{-2}. The out-of-plane angle for graphene is $\alpha = 0$ and the bond angle is $\theta = 120°$ (*i.e.* $\psi = 30°$), while the bond length and thickness of single-layer graphene can be obtained from the literature as 0.142 nm and 0.34 nm, respectively.[42] In the case of hBN, the molecular mechanics parameters k_r and k_θ can be obtained from the literature using the DREIDING force model[71] as $k_r = 4.865 \times 10^{-7}$ N nm^{-1} and $k_\theta = 6.952 \times 10^{-10}$ N nm rad^{-2}.[72] The out-of-plane angle for hBN is $\alpha = 0$ and the bond angle is $\theta = 120°$ (*i.e.* $\psi = 30°$), while the bond length and thickness of single-layer hBN can be obtained from the literature as 0.145 nm and 0.098 nm, respectively.[44] In the case of stanene, the molecular mechanics parameters k_r and k_θ can be obtained from the literature as $k_r = 0.85 \times 10^{-7}$ N nm^{-1} and $k_\theta = 1.121 \times 10^{-9}$ N nm rad^{-2}.[73,74] The out-of-plane angle for stanene is $\alpha = 17.5°$ and the bond angle is $\theta = 109°$ (*i.e.* $\psi = 35.5°$), while the bond length and thickness of single layer stanene can be obtained from the literature as 0.283 nm and 0.172 nm, respectively.[73–76] In the case of MoS_2, the molecular mechanics parameters k_r and k_θ can be obtained from the literature as $k_r = 1.646 \times 10^{-7}$ N nm^{-1} and $k_\theta = 1.677 \times 10^{-9}$ N nm rad^{-2}, while the out-of-plane angle, bond angle, bond

length and thickness of single layer MoS_2 are $\alpha = 48.15°$, $\theta = 82.92°$ (*i.e.* $\psi = 48.54°$), 0.242 nm and 0.6033 nm, respectively.[61,77–79]

3.2. Shear modulus of single-layer hexagonal nano-structures

The proposed expression for shear modulus is generalized in nature and they can be applicable for a wide range of materials having hexagonal nano-structural forms by providing respective structural parameters as input. Four different materials with hexagonal nano-structures are considered (graphene, hBN, stanene and MoS_2) that have monoplanar as well as multiplanar structural forms. Comparative results for the shear modulus is presented in Table 1 as $\bar{G}_{12} = G_{12} \times t$ with the unit TPa nm (tensile rigidity), where t is the single layer thickness.[41,44] Thus the exact numerical values of shear modulus (G_{12} in TPa) can be evaluated by dividing the presented values ($\bar{G}_{12}$ with the unit TPa nm) by the respective single-layer thickness (t in nm). It is found from the scientific literature that the shear moduli of monoplanar nanomaterials such as graphene and hBN have been investigated in previous studies (refer to Table 1), while no result for shear modulus is found for multiplanar structural forms (such as stanene and MoS_2).

Thus, to validate the proposed analytical formulae for single-layer monoplanar nanostructures, we have compared the results with available numerical values of the shear modulus in the literature. However, to validate the analytical formulae for multiplanar single-layer nanostructures, separate molecular dynamics simulation is carried out for MoS_2, which has a multiplanar nanostructure. Having the proposed closed-form formulae validated for both monoplanar as well as multiplanar nanostructures, the shear modulus is predicted for single-layer stanene having a multiplanar nanostructural form. The results of the shear modulus are presented in Table 1 for graphene, hBN, stanene and MoS_2, wherein good agreement is noted between the analytical predictions and reference results obtained from the scientific literature and molecular dynamics simulation.

The molecular dynamics simulations for the shear modulus are performed on a $10 \times 10 \times 10$ super cell for all the two-dimensional nanostructures and nano-heterostructures in LAMMPS.[85] AIREBO (adaptive intermolecular reactive empiri-

Table 1 Results for the shear modulus of single-layer materials. (Results are presented as $\bar{G}_{12} = G_{12} \times t$ (unit TPa nm), where t is the single layer thickness of a particular nanomaterial. Reference results are obtained from the literature for graphene and hBN, while separate molecular dynamics (MD) simulation is carried out for MoS_2.)

Material	Present results	Reference results
Graphene (monoplanar)	$\bar{G}_{12} = 0.1254$	0.0724–0.0741,[80] 0.1676[81] 0.0952 ± 0.0122[33]
hBN (monoplanar)	$\bar{G}_{12} = 0.0951$	0.0951,[82] 0.105,[83] 0.165[84]
Stanene (multiplanar)	$\bar{G}_{12} = 0.0325$	—
MoS_2 (multiplanar)	$\bar{G}_{12} = 0.0719$	0.079 [MD]

cal bond order) potential is used for graphene[86] and REBO (reactive empirical bond order) potential is used for MoS_2.[87] Both REBO and AIREBO potentials have been shown to accurately capture the bond–bond interaction between the carbon atoms and molybdenum–sulfur atoms for single-layer two-dimensional structures. In order to terminate the bond-order potential for the nearest neighbour interactions, a cut-off function is found to be used in most empirical potentials. We have set the cut-off parameter as 2.0 Å for the REBO part of the potential, as suggested in various previous publications.[88,89] AIREBO for graphene[90,91] and REBO for MoS_2[92,93] are found to be widely used for mechanical properties and failure analyses. It is expected to predict the shear modulus accurately; our analytical prediction gives close result with respect to the numerical values obtained from molecular dynamics simulation (refer to Table 1).

The physics-based analytical formulae presented in this paper for the shear modulus of monolayer nanostructures are capable of providing a thorough insight encompassing a wide range of materials. Variations of the shear modulus (G_{12}) with in-plane and out-of-plane angles (θ and α) for different values of the aspect ratio measure (λ) is presented in Fig. 6 using the non-dimensional parameters as described in subsection 2.5. The aspect ratio measure of the bonds (λ) varies in the range of 0.4–2.8 for common materials with hexagonal nano-structures (specifically in the case of the four considered materials: λ = 1.2507, 2.495, 0.5061, and 0.479 for graphene, hBN,

stanene and MoS_2, respectively). The results for the shear modulus is presented for λ = 0.4, 1.2, 2.0, and 2.8. Such plots can readily provide the idea about the shear modulus of any material with hexagonal nano-structures in a comprehensive manner; exact values of which can be easily obtained using the proposed computationally efficient closed-form formulae.

3.3. Elastic moduli for multi-layer hexagonal nano-heterostructures

In this section, results are provided for the shear modulus of hexagonal multi-layer nano-heterostructures. As investigations on nano-heterostructures is a new and emerging field of research, the results available for the elastic moduli of different forms of heterostructures are very scarce in the scientific literature. We have considered four different nano-heterostructures to present the results: graphene–MoS_2,[22,23] graphene–hBN,[24,25,94] graphene–stanene[26] and stanene–MoS_2[27] (belonging to the three categories as depicted in the Introduction section). Though all these four heterostructures have received attention from the concerned scientific community for different physical and chemical properties recently, only the graphene–MoS_2 heterostructure has been investigated for the Young's modulus among all the other elastic moduli.[24,25] As shear modulus of heterostructures has not been investigated yet, we have presented new results for graphene–MoS_2, graphene–hBN, graphene–stanene and stanene–
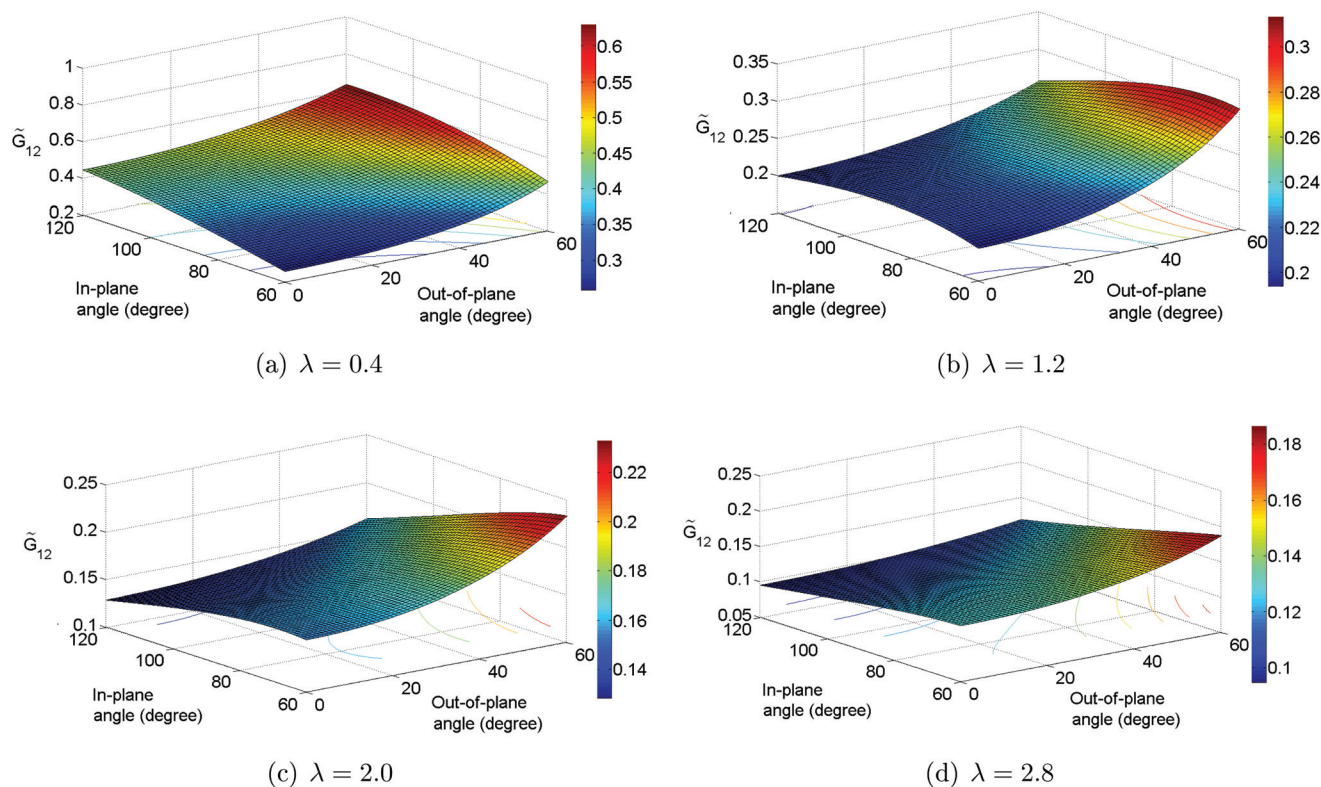

(a) $\lambda = 0.4$

(b) $\lambda = 1.2$

(c) $\lambda = 2.0$

(d) $\lambda = 2.8$

Fig. 6 Variation of shear modulus with in-plane angle (θ) and out-of-plane angle (α). Here $\lambda = \dfrac{l^2 k_r}{12 k_\theta}$, $\tilde{G}_{12} = \dfrac{G_{12} t}{k_r}$, where l and t are the bond length and single-layer thickness, respectively.

MoS_2 heterostructures based on the analytical formula presented in eqn (19).

The proposed closed-form formula (eqn (19)) for the shear modulus of nano-heterostructures is validated for different stacking sequences of graphene–MoS_2 heterostructures by carrying out separate molecular dynamics simulation (refer to Table 2). For molecular dynamics simulation of the nano-heterostructures Lennard-Jones (LJ) parameters are used for van der Waals interactions between carbon–carbon[95] and carbon–molybdenum–sulfur.[96] The LJ parameters for nano-heterostructures are verified for mechanical properties such as the Young's modulus, bending modulus, ultimate strain and fracture strength.[97] Thus, having the derived formula for the shear modulus of nano-heterostructures validated, new analytical results are presented for graphene–hBN, graphene–stanene and stanene–MoS_2 heterostructures considering different stacking sequences (refer to Table 3). The results of shear modulus corresponding to various stacking sequences are noted to have an intermediate value between the respective shear modulus for single-layer of the constituent materials, as expected on a logical basis. The derived closed-form expressions for nano-heterostructures are capable of obtaining the shear modulus corresponding to any stacking sequence of the constituent layer of nanomaterials. However, from the expressions it can be discerned that the numerical value of the shear modulus actually depends on the number of layers of different constituent materials rather than their stacking sequences. From a view-point of mechanics, this is because of the fact that the in-plane properties are not a function of the distance of individual constituent layers from the neutral plane of the entire heterostructure. The externally applied in-plane shear force is shared by the constituent layers depending on their relative individual shear stiffness. However, if other mechanical properties of the heterostructures involving the out-of-plane bending characteristics of the heterostructure are investigated, the distance of each layer from the neutral axis would be an important factor. Subsequently the out-of-plane bending characteristics will be stacking-sequence dependent properties. Fig. 7 presents the variation of the shear modulus with the number of layers of the constituent materials considering the four different nano-heterostructures. These plots can readily provide an idea about the nature of variation of the shear modulus with a stacking sequence for multi-layer nano-heterostructures in a comprehensive manner; the exact values of which can be easily obtained using the proposed computationally efficient closed-form formulae.

4. Summary and perspective

A major contribution of this article is development of the generalized closed-form formulae for the shear modulus of hexagonal single-layer materials consisting of atoms in multiple planes (i.e. multiplanar nanostructures such as stanene and MoS_2). Previous literature studies have reported the closed-form analytical formulae for the Young's moduli and Poisson's ratios of both monoplanar as well as multiplanar single layer nanostructures.[32,42–45] Recently the analytical expressions for the Young's moduli and Poisson's ratios of nano-heterostructures have been reported.[31] In the case of shear modulus, only monoplanar structures have received attention in terms of developing efficient analytical formulae,[42,44] while for multiplanar nanostructural forms, investigations related to shear modulus are very scarce, even with other approaches such as molecular dynamics simulation, *ab initio* or laboratory experiments. New results are presented in this article based on the developed analytical approach for such multiplanar nanostructures. The molecular mechanics parameters and structural geometry of different nanomaterials being well-documented in the scientific literature, the developed analytical for-

Table 2 Results for shear modulus (G_{12}, in TPa) of graphene–MoS_2 (G–M) heterostructures with different stacking sequences (the thicknesses of single-layer of graphene and MoS_2 are considered to be 0.34 nm and 0.6033 nm, respectively. Reference results are obtained from the literature (if available) and separate molecular dynamics (MD) simulation)

Configuration	Present results	Reference results
G	0.3689	0.28 ± 0.036,[33] 0.493 [81]
G/G	0.3689	0.3730 [MD]
M	0.1192	0.1310 [MD]
M/M	0.1192	0.1205 [MD]
G/M	0.2092	0.2400 [MD]
G/M/G	0.2515	0.2430 [MD]
M/G/M	0.1741	0.1685 [MD]

Table 3 Results for shear modulus (G_{12}, in TPa) of graphene–hBN (G–H), graphene–stanene (G–S) and stanene–MoS_2 (S–M) heterostructures with different stacking sequences (the single-layer thicknesses of graphene, hBN, stanene and MoS_2 are considered to be 0.34 nm, 0.33 nm, 0.172 nm and 0.6033 nm, respectively)

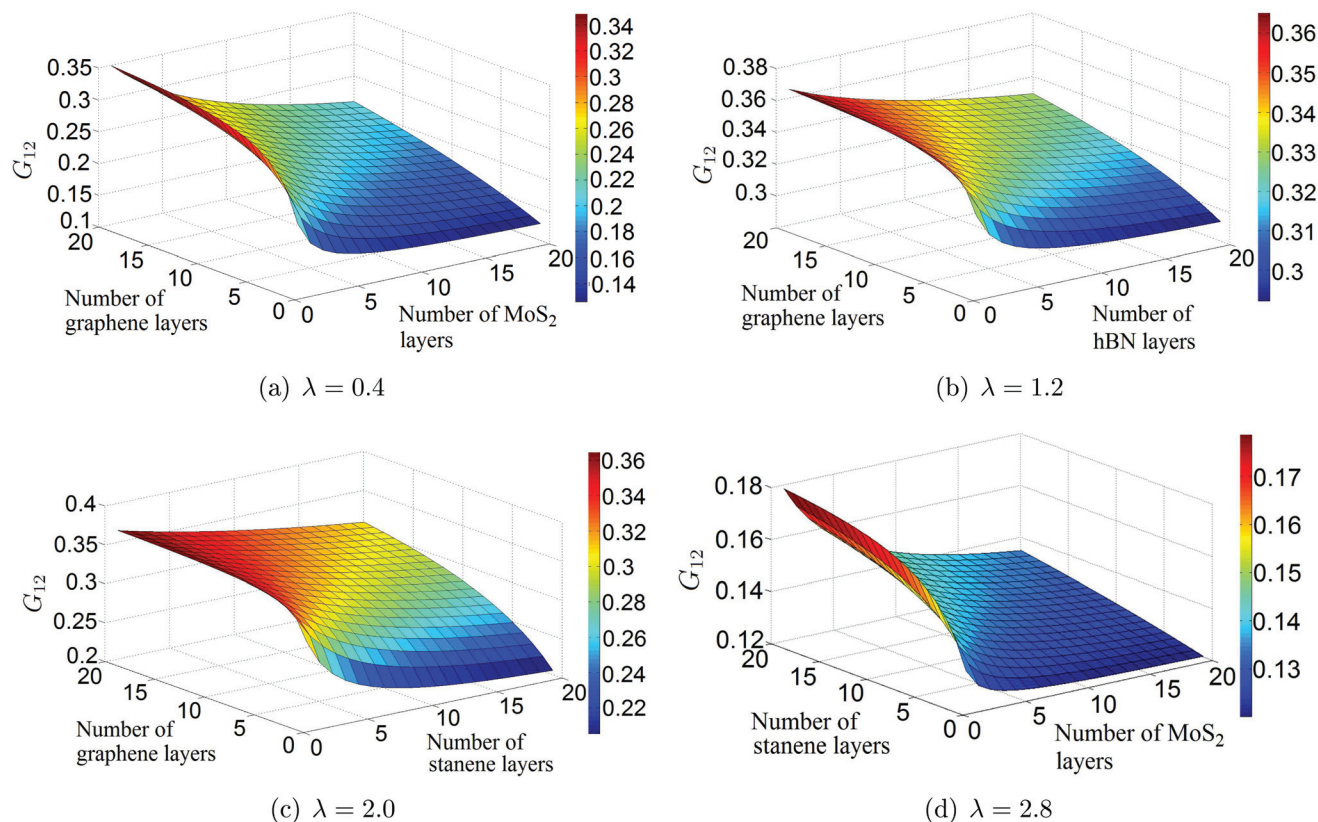| G–H heterostructures		G–S heterostructures		S–M heterostructures	
Configuration	G_{12}	Configuration	G_{12}	Configuration	G_{12}
G	0.3689	G	0.3689	S	0.1890
G/G	0.3689	G/G	0.3689	S/S	0.1890
H	0.2883	S	0.1890	M	0.1192
H/H	0.2883	S/S	0.1890	M/M	0.1192
G/H	0.3292	G/S	0.3085	S/M	0.1347
G/H/G	0.3426	G/S/G	0.3326	S/M/S	0.1446
H/G/H	0.3157	S/G/S	0.2784	M/S/M	0.1279

Fig. 7 Variation of shear modulus (G_{12}) with the number of layers in (a) graphene–MoS$_2$ heterostructure, (b) graphene–hBN heterostructure, (c) graphene–stanene heterostructure and (d) stanene–MoS$_2$ heterostructure.

mulae for shear modulus can be applied for a wide range of nanostructures. The formulae for hexagonal nanostructures can be readily extended to other forms of nanostructures such as multiplanar square or rectangular forms.[98] Nano-heterostructures being a new field of investigation, results are available only for the Young's moduli of graphene–MoS$_2$ heterostructures based on molecular dynamics simulation. We have presented new results for the shear modulus of four different nano-heterostructures (graphene–MoS$_2$, graphene–hBN, graphene–stanene and stanene–MoS$_2$).

Mechanical properties such as the Young's moduli, shear modulus and Poisson's ratios are of utmost importance for accessing the viability of a material's use in various applications of nanoelectromechanical systems. Shear modulus assumes a crucial role in determining the resonance frequency of vibration modes involving torsion, which have been reported to have advantage over flexural modes due to the absence of thermoelastic loss leading to an improvement in mechanical quality factors and device sensitivity parameters. Shear deformation characteristics are also important in the wrinkling and rippling behaviour of two-dimensional materials that control the charge carrier scattering properties and electron mobility.[33] The formulae for the shear modulus of nanostructures and nano-heterostructures presented in this article can serve as an efficient reference for any nano-scale material having a hexagonal structural form. The expressions

for obtaining the shear modulus of nano-heterostructures are applicable for any stacking sequence of the constituent single layers. Even though results are presented in this article considering only two different constituent materials, the proposed formulae can be used for heterostructures containing any number of different materials.[28] A noteworthy feature of the presented expressions is the computational efficiency and cost-effectiveness compared to performing molecular dynamics simulation or nano-scale experiments. Such development can help bring about the much-needed impetus in the research of two-dimensional materials, which is often hindered due to the need for carrying out computationally expensive and time consuming simulations/laboratory experiments and availability of interatomic potentials. Besides deterministic analysis of shear moduli, as presented in this paper, the efficient closed-form formulae could be an attractive option for carrying out uncertainty analysis[99–104] following a Monte Carlo simulation based approach.

After several years of intensive study, graphene research has logically reached a rather mature stage. Thus investigations of various other two-dimensional and quasi-two-dimensional materials have started receiving due attention recently. The possibility of combining single layers of different 2D materials has expanded this field of research dramatically; well beyond the scope of considering a simple single layer graphene or other 2D materials. The interest in such heterostructures is

growing very rapidly with the advancement of synthesizing such materials in the laboratory, similar to the considerable amount of research on graphene observed about a decade ago. The attentiveness is expected to expand further in coming years with the possibility of considering different nanoelectro-mechanical properties of prospective combinations (single and multi-layer structures with different stacking sequences) of a number of 2D materials. This, in turn introduces the possibility of opening a new dimension of application-specific material development (metamaterial) at the nano-scale. The efficient closed-form expressions developed in this paper will provide a ready reference for the shear modulus of such heterostructures.

5. Conclusion

Generalized closed-form analytical formulae for the shear modulus of hexagonal multiplanar nano-structures and nano-heterostructures are developed based on a physics-based analytical approach. The dependence of shear modulus on bond length, bond angles and bond strength parameters is explicitly demonstrated. Four different single-layered materials having monoplanar as well as multiplanar structural forms (graphene, hBN, stanene and MoS_2) and four different nano-heterostructures (graphene–MoS_2, graphene–hBN, graphene–stanene and stanene–MoS_2) are considered to present results based on the analytical approach. Good agreement between the results obtained from the derived analytical expressions and the results obtained from the scientific literature (as available) or separate molecular dynamics simulations corroborates the validity of the proposed formulae. The physics-based analytical formulae are capable of providing a comprehensive in-depth insight regarding the behaviour of multiplanar hexagonal nano-structures and heterostructures under shear deformation. The effects of variation in in-plane and out-of-plane angles on the shear modulus of materials are investigated using the closed-form formulae based on non-dimensional parameters. In the case of nano-heterostructures, the variation of shear modulus is presented with the number of layers of the constituent materials.

The concept to develop expressions for hexagonal nano-heterostructures can be extended to other forms of nano-structures in the future. The attractive feature of the developed analytical approach is that it is computationally efficient, physically insightful and easy to implement, yet yields accurate results. As the proposed formulae are general in nature and applicable to a wide range of materials and their combinations with hexagonal nano-structures, they can play a crucial role in characterizing material properties in future nano-material development.

Conflicts of interest

There are no conflicts to declare.

Acknowledgements

References

1 K. Novoselov, A. K. Geim, S. Morozov, D. Jiang, M. Katsnelson, I. Grigorieva, S. Dubonos and A. Firsov, Two-dimensional gas of massless dirac fermions in graphene, *Nature*, 2005, **438**(7065), 197–200.

2 Y. Pan, L. Zhang, L. Huang, L. Li, L. Meng, M. Gao, Q. Huan, X. Lin, Y. Wang, S. Du, *et al.* Construction of 2d atomic crystals on transition metal surfaces, graphene, silicene, and hafnene, *Small*, 2014, **10**(11), 2215–2225.

3 S. Balendhran, S. Walia, H. Nili, S. Sriram and M. Bhaskaran, Elemental analogues of graphene, silicene, germanene, stanene, and phosphorene, *Small*, 2015, **11**(6), 640–652.

4 M. Xu, T. Liang, M. Shi and H. Chen, Graphene–like two–dimensional materials, *Chem. Rev.*, 2013, **113**(5), 3766–3798.

5 S. Das, J. A. Robinson, M. Dubey, H. Terrones and M. Terrones, Beyond grapheneProgress in novel two-dimensional materials and van der Waals solids, *Annu. Rev. Mater. Res.*, 2015, **45**, 1–27.

6 F. Schwierz, J. Pezoldt and R. Granzner, Two-dimensional materials and their prospects in transistor electronics, *Nanoscale*, 2015, **7**, 8261–8283.

7 P. Chakraborty, T. Das, D. Nafday, L. Boeri and T. Saha-Dasgupta, Manipulating the mechanical properties of ti$_2$C mxene, Effect of substitutional doping, *Phys. Rev. B*, 2017, **95**, 184106.

8 M. Ghorbani-Asl, S. Borini, A. Kuc and T. Heine, Strain-dependent modulation of conductivity in single-layer transition-metal dichalcogenides, *Phys. Rev. B: Condens. Matter Mater. Phys.*, 2013, **87**, 235434.

9 H. Wang, H. Feng and J. Li, Graphene and graphene-like layered transition metal dichalcogenides in energy conversion and storage, *Small*, 2014, **10**(11), 2165–2181.

10 A. A. Balandin, S. Ghosh, W. Bao, I. Calizo, D. Teweldebrhan, F. Miao and C. N. Lau, Superior thermal conductivity of single-layer graphene, *Nano Lett.*, 2008, **8**(3), 902–907.

11 A. K. Geim and I. V. Grigorieva, Van der waals hetero-structures, *Nature*, 2013, **499**(7459), 419–425.

12 Y. J. Zhang, M. Yoshida, R. Suzuki and Y. Iwasa, 2d crystals of transition metal dichalcogenide and their iontronic functionalities, *2D Mater.*, 2015, **2**(4), 044004.

13 B. van den Broek, M. Houssa, A. Lu, G. Pourtois, V. Afanas'ev and A. Stesmans, Silicene nanoribbons on transition metal dichalcogenide substrates, Effects on

electronic structure and ballistic transport, *Nano Res.*, 2016, **9**(11), 3394–3406.

14 M. Houssa, B. van den Broek, K. Iordanidou, A. K. A. Lu, G. Pourtois, J.-P. Locquet, V. Afanas'ev and A. Stesmans, Topological to trivial insulating phase transition in stanene, *Nano Res.*, 2016, **9**(3), 774–778.

15 Z. Shi and C. V. Singh, The ideal strength of two-dimensional stanene may reach or exceed the griffith strength estimate, *Nanoscale*, 2017, **9**, 7055–7062.

16 F. Ersan, S. Cahangirov, G. Gökoğlu, A. Rubio and E. Aktürk, Stable monolayer honeycomb-like structures of Ru X_2(x = S, Se), *Phys. Rev. B*, 2016, **94**, 155415.

17 M.-Y. Li, C.-H. Chen, Y. Shi and L.-J. Li, Heterostructures based on two-dimensional layered materials and their potential applications, *Mater. Today*, 2016, **19**(6), 322–335.

18 Q. Peng, K. Hu, B. Sa, J. Zhou, B. Wu, X. Hou and Z. Sun, Unexpected elastic isotropy in a black phosphorene/tic2 van der Waals heterostructure with flexible li-ion battery anode applications, *Nano Res.*, 2017, **10**(9), 3136–3150.

19 X. Liu, J. Gao, G. Zhang and Y.-W. Zhang, Mos2-graphene in-plane contact for high interfacial thermal conduction, *Nano Res.*, 2017, **10**(9), 2944–2953.

20 H. Wang, F. Liu, W. Fu, Z. Fang, W. Zhou and Z. Liu, Two-dimensional heterostructures: fabrication, characterization, and application, *Nanoscale*, 2014, **6**, 12250–12272.

21 R. M. Elder, M. R. Neupane and T. L. Chantawansri, Stacking order dependent mechanical properties of graphene/mos2 bilayer and trilayer heterostructures, *Appl. Phys. Lett.*, 2015, **107**(7), 073101.

22 K. Liu, Q. Yan, M. Chen, W. Fan, Y. Sun, J. Suh, D. Fu, S. Lee, J. Zhou, S. Tongay, J. Ji, J. B. Neaton and J. Wu, Elastic properties of chemical-vapor-deposited monolayer mos2, ws2, and their bilayer heterostructures, *Nano Lett.*, 2014, **14**(9), 5097–5103.

23 J.-W. Jiang and H. S. Park, Mechanical properties of mos2/graphene heterostructures, *Appl. Phys. Lett.*, 2014, **105**(3), 033108.

24 C. Zhang, S. Zhao, C. Jin, A. L. Koh, Y. Zhou, W. Xu, Q. Li, Q. Xiong, H. Peng and Z. Liu, Direct growth of large-area graphene and boron nitride heterostructures by a co-segregation method, *Nat. Commun.*, 2015, **6**, 6519.

25 Q. Li, M. Liu, Y. Zhang and Z. Liu, Hexagonal boron nitride–graphene heterostructures: Synthesis and interfacial properties, *Small*, 2016, **12**(1), 32–50.

26 X. Chen, R. Meng, J. Jiang, Q. Liang, Q. Yang, C. Tan, X. Sun, S. Zhang and T. Ren, Electronic structure and optical properties of graphene/stanene heterobilayer, *Phys. Chem. Chem. Phys.*, 2016, **18**(24), 16302–16309.

27 C.-C. Ren, Y. Feng, S.-F. Zhang, C.-W. Zhang and P.-J. Wang, The electronic properties of the stanene/mos2 heterostructure under strain, *RSC Adv.*, 2017, **7**, 9176–9181.

28 X. Wang and F. Xia, Van der Waals heterostructures: stacked 2d materials shed light, *Nat. Mater.*, 2015, **14**(3), 264–265.

29 S. Entani, L. Y. Antipina, P. V. Avramov, M. Ohtomo, Y. Matsumoto, N. Hirao, I. Shimoyama, H. Naramoto, Y. Baba, P. B. Sorokin and S. Sakai, Contracted interlayer distance in graphene/sapphire heterostructure, *Nano Res.*, 2015, **8**(5), 1535–1545.

30 L. Wang, X. Zhou, T. Ma, D. Liu, L. Gao, X. Li, J. Zhang, Y. Hu, H. Wang, Y. Dai and J. Luo, Superlubricity of a graphene/mos2 heterostructure: a combined experimental and dft study, *Nanoscale*, 2017, **9**, 10846–10853.

31 T. Mukhopadhyay, A. Mahata, S. Adhikari and M. A. Zaeem, Effective mechanical properties of multilayer nano-heterostructures, *Sci. Rep.*, 2017, **7**, 15818.

32 T. Mukhopadhyay, A. Mahata, S. Adhikari and M. A. Zaeem, Effective elastic properties of two dimensional multiplanar hexagonal nanostructures, *2D Mater.*, 2017, **4**(2), 025006.

33 X. Liu, T. H. Metcalf, J. T. Robinson, B. H. Houston and F. Scarpa, Shear modulus of monolayer graphene prepared by chemical vapor deposition, *Nano Lett.*, 2012, **12**(2), 1013–1017.

34 V. Zolyomi, J. R. Wallbank and V. I. Fal'ko, Silicane and germanane: tight-binding and first-principles studies, *2D Mater.*, 2014, **1**(1), 011005.

35 T. Lorenz, J.-O. Joswig and G. Seifert, Stretching and breaking of monolayer mos2 – an atomistic simulation, *2D Mater.*, 2014, **1**(1), 011007.

36 F. Liu, P. Ming and J. Li, Ab initio calculation of ideal strength and phonon instability of graphene under tension, *Phys. Rev. B: Condens. Matter Mater. Phys.*, 2007, **76**(6), 064120.

37 L. Debbichi, H. Kim, T. Björkman, O. Eriksson and S. Lebègue, First-principles investigation of two-dimensional trichalcogenide and sesquichalcogenide monolayers, *Phys. Rev. B*, 2016, **93**, 245307.

38 S. Lebègue and O. Eriksson, Electronic structure of two-dimensional crystals from ab initio theory, *Phys. Rev. B: Condens. Matter Mater. Phys.*, 2009, **79**, 115409.

39 M. J. Cherukara, B. Narayanan, A. Kinaci, K. Sasikumar, S. K. Gray, M. K. Chan and S. K. R. S. Sankaranarayanan, Ab initio-based bond order potential to investigate low thermal conductivity of stanene nanostructures, *J. Phys. Chem. Lett.*, 2016, **7**(19), 3752–3759.

40 R. Grantab, V. B. Shenoy and R. S. Ruoff, Anomalous strength characteristics of tilt grain boundaries in graphene, *Science*, 2010, **330**(6006), 946–948.

41 T. Chang and H. Gao, Size-dependent elastic properties of a single-walled carbon nanotube via a molecular mechanics model, *J. Mech. Phys. Solids*, 2003, **51**(6), 1059–1074.

42 F. Scarpa, S. Adhikari and A. S. Phani, Effective elastic mechanical properties of single layer graphene sheets, *Nanotechnology*, 2009, **20**(6), 065709.

43 M. M. Shokrieh and R. Rafiee, Prediction of Young's modulus of graphene sheets and carbon nanotubes using nanoscale continuum mechanics approach, *Mater. Des.*, 2010, **31**, 790–795.

44 L. Boldrin, F. Scarpa, R. Chowdhury and S. Adhikari, Effective mechanical properties of hexagonal boron nitride nanosheets, *Nanotechnology*, 2011, **22**(50), 505702.

45 M.-Q. Le, Prediction of young's modulus of hexagonal monolayer sheets based on molecular mechanics, *Int. J. Mech. Mater. Des.*, 2015, **11**(1), 15–24.

46 Y. Li, W. Zhang, B. Guo and D. Datta, Interlayer shear of nanomaterials: Graphene–graphene, boron nitride–boron nitride and graphene–boron nitride, *Acta Mech. Solida Sin.*, 2017, **30**(3), 234–240.

47 B. R. Gelin, *Molecular Modeling of Polymer Structures and Properties*, Hanser Gardner Publications, 1994.

48 J. Zhang and C. Wang, Free vibration analysis of micro-tubules based on the molecular mechanics and continuum beam theory, *Biomech. Model. Mechanobiol.*, 2016, **15**(5), 1069–1078.

49 L. Gibson and M. F. Ashby, *Cellular Solids Structure and Properties*, Cambridge University Press, Cambridge, UK, 1999.

50 T. Mukhopadhyay and S. Adhikari, Equivalent in-plane elastic properties of irregular honeycombs: An analytical approach, *Int. J. Solids Struct.*, 2016, **91**, 169–184.

51 T. Mukhopadhyay and S. Adhikari, Effective in-plane elastic properties of auxetic honeycombs with spatial irregularity, *Mech. Mater.*, 2016, **95**, 204–222.

52 T. Mukhopadhyay and S. Adhikari, Free vibration analysis of sandwich panels with randomly irregular honeycomb core, *J. Eng. Mech.*, 2016, 06016008, DOI: 0.1061/(ASCE) EM.1943-7889.0001153.

53 T. Mukhopadhyay and S. Adhikari, Stochastic mechanics of metamaterials, *Compos. Struct.*, 2017, **162**, 85–97.

54 T. Mukhopadhyay, S. Adhikari and A. Batou, Frequency domain homogenization for the viscoelastic properties of spatially correlated quasi-periodic lattices, *Int. J. Mech. Sci.*, 2017, DOI: 10.1016/j.ijmecsci.2017.09.004.

55 T. Mukhopadhyay and S. Adhikari, Effective in-plane elastic moduli of quasi-random spatially irregular hexagonal lattices, *Int. J. Eng. Sci.*, 2017, **119**, 142–179.

56 C. Huang, C. Chen, M. Zhang, L. Lin, X. Ye, S. Lin, M. Antonietti and X. Wang, Carbon-doped bn nanosheets for metal-free photoredox catalysis, *Nat. Commun.*, 2015, **6**, 7698.

57 F. Zhu, W. Chen, Y. Xu, C. Gao, D. Guan, C. Liu, D. Qian, S. Zhang and J. Jia, Epitaxial growth of two-dimensional stanene, *Nat. Mater.*, 2015, **14**(10), 1020–1025.

58 Z. Ni, Q. Liu, K. Tang, J. Zheng, J. Zhou, R. Qin, Z. Gao, D. Yu and J. Lu, Tunable bandgap in silicene and germanene, *Nano Lett.*, 2012, **12**(1), 113–118.

59 H. Liu, A. T. Neal, Z. Zhu, Z. Luo, X. Xu, D. Tomanek and P. D. Ye, Phosphorene: An unexplored 2d semiconductor with a high hole mobility, *ACS Nano*, 2014, **8**(4), 4033–4041.

60 A. J. Mannix, X. Zhou, B. Kiraly, J. D. Wood, D. Alducin, B. D. Myers, X. Liu, B. L. Fisher, U. Santiago, J. R. Guest, M. J. Yacaman, A. Ponce, A. R. Oganov, M. C. Hersam and N. P. Guisinger, Synthesis of borophenes: Anisotropic, two-dimensional boron polymorphs, *Science*, 2015, **350**(6267), 1513–1516.

61 T. M. Brunier, M. G. B. Drew and P. C. H. Mitchell, Molecular mechanics studies of molybdenum disulphide catalysts parameterisation of molybdenum and sulphur, *Mol. Simul.*, 1992, **9**(2), 143–159.

62 R. C. Cooper, C. Lee, C. A. Marianetti, X. Wei, J. Hone and J. W. Kysar, Nonlinear elastic behavior of two-dimensional molybdenum disulfide, *Phys. Rev. B: Condens. Matter Mater. Phys.*, 2013, **87**, 035423.

63 S. Balendhran, J. Z. Ou, M. Bhaskaran, S. Sriram, S. Ippolito, Z. Vasic, E. Kats, S. Bhargava, S. Zhuiykov and K. Kalantar-zadeh, Atomically thin layers of mos2 via a two step thermal evaporation-exfoliation method, *Nanoscale*, 2012, **4**, 461–466.

64 W. Zhao, Z. Ghorannevis, L. Chu, M. Toh, C. Kloc, P.-H. Tan and G. Eda, Evolution of electronic structure in atomically thin sheets of ws2 and wse2, *ACS Nano*, 2013, **7**(1), 791–797.

65 R. Coehoorn, C. Haas, J. Dijkstra, C. J. F. Flipse, R. A. de Groot and A. Wold, Electronic structure of mose$_2$, mos$_2$, and wse$_2$. i. band-structure calculations and photoelectron spectroscopy, *Phys. Rev. B: Condens. Matter Mater. Phys.*, 1987, **35**, 6195–6202.

66 C. Ruppert, O. B. Aslan and T. F. Heinz, Optical properties and band gap of single- and few-layer mote2 crystals, *Nano Lett.*, 2014, **14**(11), 6231–6236.

67 S. Bruzzone, D. Logoteta, G. Fiori and G. Iannaccone, Vertical transport in graphene-hexagonal boron nitride heterostructure devices, *Sci. Rep.*, 2015, **5**, 14519.

68 Y. Cai, G. Zhang and Y.-W. Zhang, Electronic properties of phosphorene/graphene and phosphorene/hexagonal boron nitride heterostructures, *J. Phys. Chem. C*, 2015, **119**(24), 13929–13936.

69 C. Li and T. W. Chou, A structural mechanics approach for the analysis of carbon nanotubes, *Int. J. Solids Struct.*, 2003, **40**(10), 2487–2499.

70 W. D. Cornell, P. Cieplak, C. I. Bayly, I. R. Gould, K. M. Merz, D. M. Ferguson, D. C. Spellmeyer, T. Fox, J. W. Caldwell and P. A. Kollman, A second generation force field for the simulation of proteins, nucleic acids, and organic molecules, *J. Am. Chem. Soc.*, 1995, **117**(19), 5179–5197.

71 S. L. Mayo, B. D. Olafson and W. A. Goddard, Dreiding: a generic force field for molecular simulations, *J. Phys. Chem.*, 1990, **94**(26), 8897–8909.

72 C. Li and T.-W. Chou, Static and dynamic properties of single-walled boron nitride nanotubes, *J. Nanosci. Nanotechnol.*, 2006, **6**(1), 54–60.

73 M. Modarresi, A. Kakoee, Y. Mogulkoc and M. Roknabadi, Effect of external strain on electronic structure of stanene, *Comput. Mater. Sci.*, 2015, **101**, 164–167.

74 D. Wang, L. Chen, X. Wang, G. Cui and P. Zhang, The effect of substrate and external strain on electronic struc-

tures of stanene film, *Phys. Chem. Chem. Phys.*, 2015, **17**, 26979–26987.

75 P. Tang, P. Chen, W. Cao, H. Huang, S. Cahangirov, L. Xian, Y. Xu, S.-C. Zhang, W. Duan and A. Rubio, Stable two-dimensional dumbbell stanene: A quantum spin hall insulator, *Phys. Rev. B: Condens. Matter Mater. Phys.*, 2014, **90**, 121408.

76 B. van den Broek, M. Houssa, E. Scalise, G. Pourtois, V. V. Afanasev and A. Stesmans, Two-dimensional hexagonal tin: ab initio geometry, stability, electronic structure and functionalization, *2D Mater.*, 2014, **1**(2), 021004.

77 K. Bronsema, J. De Boer and F. Jellinek, On the structure of molybdenum diselenide and disulfide, *Z. Anorg. Allg. Chem.*, 1986, **540**(9–10), 15–17.

78 T. Wieting and J. Verble, Infrared and raman studies of long-wavelength optical phonons in hexagonal mos2, *Phys. Rev. B: Condens. Matter Mater. Phys.*, 1971, **3**(12), 4286.

79 Z. Ma and S. Dai, Ab initio studies on the electronic structure of the complexes containing mo–s bond using relativistic effective core potentials, *Acta Chim. Sin. (Engl. Ed.)*, 1989, **7**(3), 201–208.

80 A. Sakhaee-Pour, Elastic properties of single layered graphene sheet, *Solid State Commun.*, 2009, **149**, 91–95.

81 K. V. Zakharchenko, M. I. Katsnelson and A. Fasolino, Finite temperature lattice properties of graphene beyond the quasiharmonic approximation, Phys, *Rev. Lett.*, 2009, **102**, 046808.

82 L. Jiang and W. Guo, A molecular mechanics study on size-dependent elastic properties of single-walled boron nitride nanotubes, *J. Mech. Phys. Solids*, 2011, **59**(6), 1204–1213.

83 A. Bosak, J. Serrano, M. Krisch, K. Watanabe, T. Taniguchi and H. Kanda, Elasticity of hexagonal boron nitride: Inelastic x-ray scattering measurements, *Phys. Rev. B: Condens. Matter Mater. Phys.*, 2006, **73**, 041402.

84 V. Verma, V. K. Jindal and K. Dharamvir, Elastic moduli of a boron nitride nanotube, *Nanotechnology*, 2007, **18**(43), 435711.

85 S. Plimpton, Fast parallel algorithms for short-range molecular dynamics, *J. Comput. Phys.*, 1995, **117**(1), 1–19.

86 D. W. Brenner, O. A. Shenderova, J. A. Harrison, S. J. Stuart, B. Ni and S. B. Sinnott, A second-generation reactive empirical bond order (rebo) potential energy expression for hydrocarbons, *J. Phys.: Condens. Matter*, 2002, **14**(4), 783.

87 T. Liang, S. R. Phillpot and S. B. Sinnott, Parametrization of a reactive many-body potential for mo–s systems, *Phys. Rev. B: Condens. Matter Mater. Phys.*, 2009, **79**(24), 245110.

88 O. Shenderova, D. Brenner, A. Omeltchenko, X. Su and L. Yang, Atomistic modeling of the fracture of polycrystalline diamond, *Phys. Rev. B: Condens. Matter Mater. Phys.*, 2000, **61**(6), 3877.

89 H. Zhao, K. Min and N. Aluru, Size and chirality dependent elastic properties of graphene nanoribbons under uniaxial tension, *Nano Lett.*, 2009, **9**(8), 3012–3015.

90 J.-W. Jiang, J.-S. Wang and B. Li, Young's modulus of graphene: a molecular dynamics study, *Phys. Rev. B: Condens. Matter Mater. Phys.*, 2009, **80**(11), 113405.

91 J. Xiao, J. Staniszewski and J. Gillespie, Fracture and progressive failure of defective graphene sheets and carbon nanotubes, *Compos. Struct.*, 2009, **88**(4), 602–609.

92 J. A. Stewart and D. Spearot, Atomistic simulations of nanoindentation on the basal plane of crystalline molybdenum disulfide(mos2), *Modell. Simul. Mater. Sci. Eng.*, 2013, **21**(4), 045003.

93 M. Li, Y. Wan, L. Tu, Y. Yang and J. Lou, The effect of v mos3 point defect on the elastic properties of monolayer mos2 with rebo potentials, *Nanoscale Res. Lett.*, 2016, **11**(1), 155.

94 C.-C. Chen, Z. Li, L. Shi and S. B. Cronin, Thermoelectric transport across graphene/hexagonal boron nitride/graphene heterostructures, *Nano Res.*, 2015, **8**(2), 666–672.

95 M. Neek-Amal and F. Peeters, Nanoindentation of a circular sheet of bilayer graphene, *Phys. Rev. B: Condens. Matter Mater. Phys.*, 2010, **81**(23), 235421.

96 J.-W. Jiang and H. S. Park, Mechanical properties of mos2/graphene heterostructures, *Appl. Phys. Lett.*, 2014, **105**(3), 033108.

97 R. M. Elder, M. R. Neupane and T. L. Chantawansri, Stacking order dependent mechanical properties of graphene/mos2 bilayer and trilayer heterostructures, *Appl. Phys. Lett.*, 2015, **107**(7), 073101.

98 V. Sorkin and Y. W. Zhang, The structure and elastic properties of phosphorene edges, *Nanotechnology*, 2015, **26**(23), 235707.

99 T. Mukhopadhyay, T. Mahata, S. Dey and S. Adhikari, Probabilistic analysis and design of hcp nanowires: An efficient surrogate based molecular dynamics simulation approach, *J. Mater. Sci. Technol.*, 2016, **32**(12), 1345–1351.

100 A. Mahata, T. Mukhopadhyay and S. Adhikari, A polynomial chaos expansion based molecular dynamics study for probabilistic strength analysis of nano-twinned copper, *Mater. Res. Express*, 2016, **3**(3), 036501.

101 S. Naskar, T. Mukhopadhyay, S. Sriramula and S. Adhikari, Stochastic natural frequency analysis of damaged thin-walled laminated composite beams with uncertainty in micromechanical properties, *Compos. Struct.*, 2017, **160**, 312–334.

102 S. Dey, T. Mukhopadhyay, S. Naskar, T. Dey, H. Chalak and S. Adhikari, Probabilistic characterisation for dynamics and stability of laminated soft core sandwich plates, *J. Sandwich Struct. Mater.*, DOI: 10.1177/1099636217694229.

103 S. Dey, T. Mukhopadhyay, S. Sahu and S. Adhikari, Stochastic dynamic stability analysis of composite curved panels subjected to non-uniform partial edge loading, *Eur. J. Mech. A-Solid.*, 2018, **67**, 108–122.

104 S. Dey, T. Mukhopadhyay, S. Sahu and S. Adhikari, Effect of cutout on stochastic natural frequency of composite curved panels, *Composites, Part B*, 2016, **105**, 188–202.